

DEFORMATION OF SANDSTONE IN MESO-SCALE HYPERVELOCITY CRATERING EXPERIMENTS. T. Kenkmann¹, M. Patzschke¹, K. Thoma², F. Schäfer², K. Wünnemann¹, A. Deutsch³, and the MEMIN-team⁴; ¹Museum of Natural History, Humboldt-University Berlin, Invalidenstrasse 43, 10115 Berlin, Germany, Thomas.kenkmann@museum.hu-berlin.de, ²EMI-Freiburg Efringenkirchen, Germany, thoma@fhg-emi.de, ³WWU Münster, Germany ⁴MEMIN-Team

Introduction: Meteorite impacts on porous sandstones and regoliths are frequent in the solar system. Studies of shock processes and high strain deformation on such rocks have been carried out, e.g. at Meteor crater [1, 2] or Upheaval Dome [3]. Here, we present results from cratering experiments on sandstone [4, 5] and discuss the progressive deformation of sandstone with increasing distance to the point of impact (Fig. 1).

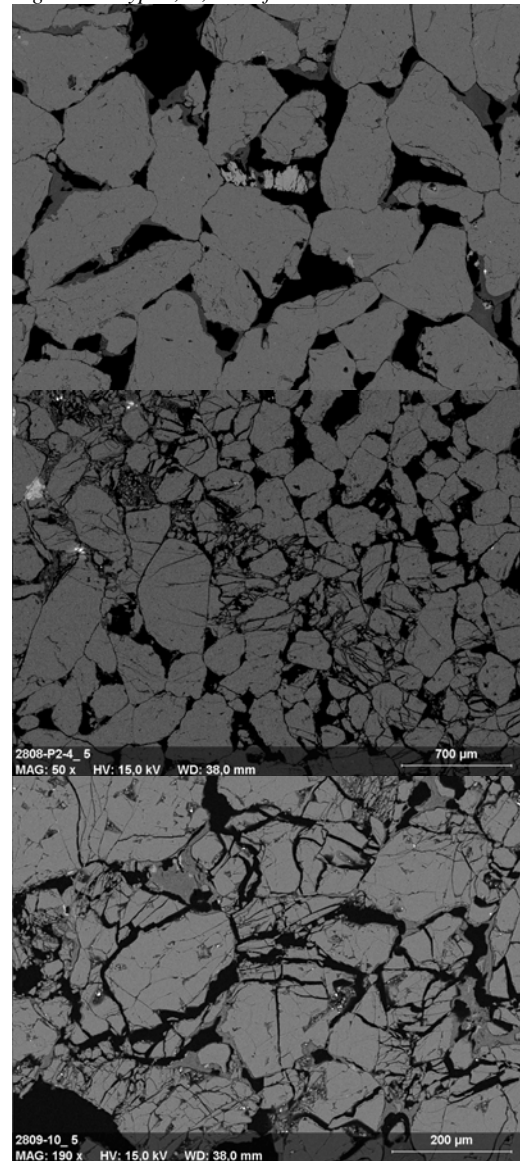
Experiments: Two experiments have been carried out with a two-stage light gas gun (EMI-Freiburg) [6]. We used steel spheres (10 mm Ø, 4.1 g) accelerated to $\sim 5300 \text{ ms}^{-1}$ as projectiles and Seeberger sandstone (block size: 100 x 100 x 50cm, grain size: 169 \pm 8 μm ; porosity: 12-20vol.%) as target material. The experiments were performed under dry (*Exp. 2808*) and wet (*Exp. 2809*; ~ 44 vol% water saturation) conditions.

Results: The experimentally produced craters in dry and wet sandstone differ strongly in diameter, depth, depth/diameter ratio, volume, and shape (Figs. 2-3)[4, 5]. Both craters are enlarged by spallation and fracturing. Transient crater diameters of 8.2 and 11.3 cm are estimated for the dry and wet crater, respectively [4; 5]. Cross sections through the craters (Fig. 2) and plane view analysis of outcropping fracture zones (Fig. 4) show that most fractures strike concentrically and dip at shallow angle, and extend sideways as tensile faults in both experiments. Bedding planes are preferential sites for strain localization. These fracture zones in combination with radial fractures (Fig. 4) delineate spall plates. They were ejected more extensively in the wet target experiment and led to a larger final crater size. Deformation beneath the crater is restricted to a ~ 3 cm deep zone. Microstructural analysis of ejected sandstone fragments and of samples from underneath the crater floor at varying distances led to the discrimination of three types of deformation in both experiments: Type I (Fig. 1a): virtually undeformed sandstone with intact porosity and no shock indication. Type I occurs ubiquitously underneath the crater and reaches close to the crater floor surface. Type II (Fig. 1b): Localized brittle fracturing in otherwise weakly-to-undeformed sandstone with intact porosity. Within ~ 1 mm wide shear zones intragranular fracturing, grain size reduction, and pore space collapse occurs; shock features have not been observed. Type II occurs where fracture zones are situated (Fig. 2) and is more frequent near the crater floor surface, but also occurs in ejected clasts. Type III (Fig.1c):

Intensive intragranular fracturing affects the entire rock, and leads to penetrative pore space crushing and cataclastic flow. Single grains often appear chopped along subparallel fractures. Fractures are occasionally filled with projectile metal or mobilized phyllosilicates that originally coated quartz grains. Type III is found in the ejecta and decorating the crater floor surface.

Discussion: A transition from Type II to Type III deformation is indicated by progressively closer spaced brittle fracture networks. As all grain-to-grain contacts are crushed in Type III material, there is no more

Fig. 1 a-c. Type I, II, III deformation in sandstone



cohesion and the material will be ejected. Differences in crater shape of the dry and wet target can be attributed to different volumes of Type III cataclastically deformed sandstone. The zone of pervasive cataclastic flow reaches deeper in the dry experiment because pore space collapse is not impeded by pore fluids.

References: [1] Kieffer et al., 1976. *Con. Min. Petrol* 59, 41-93. [2] Kieffer, Simonds., 1980. *Rev Geophys Space Phys*, 18, 143-181. [3] Kenkmann, 2003. *EPSL* 214, 43-58 [4] Kenkmann et al., 2006. *LPSC* 37#1587 [5] Wünnemann et al. 2006. *ESTEC-Conf. Nordwijk*. [6] Schäfer, et al 2006. *ESA SP-612*

Fig. 3a Gypsum mold of crater Exp 2808

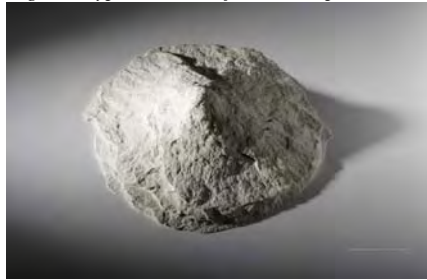


Fig. 3b Exp. 2809

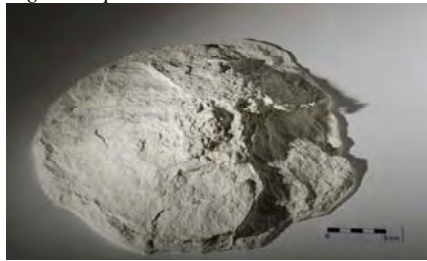


Fig. 2

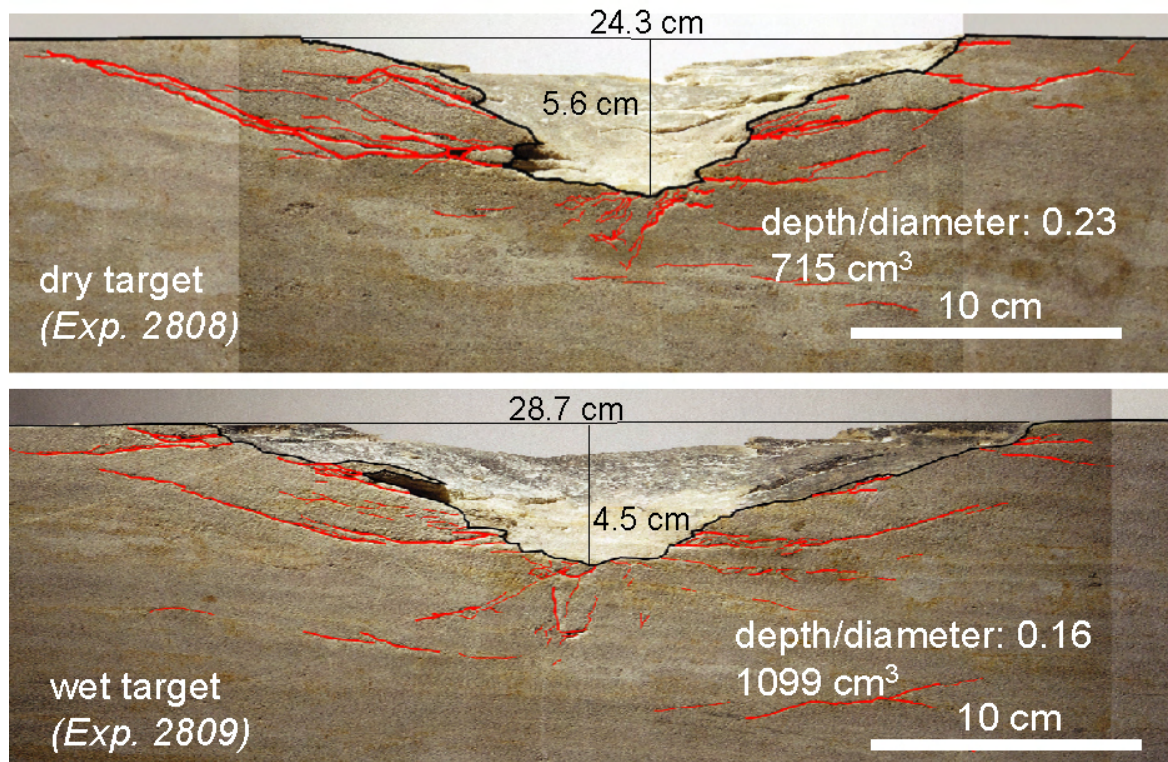


Fig. 4a Fractures in plane view, Exp. 2808

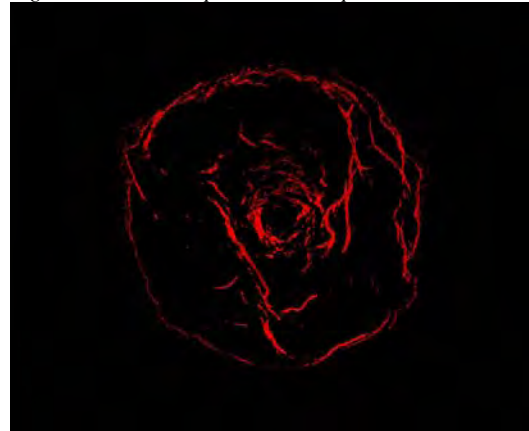


Fig. 4b Exp. 2809

